Proceedings of the Fifteenth International Conference on
Computational Structures Technology
Edited by: P. Iványi, J. Kruis and B.H.V. Topping
Civil-Comp Conferences, Volume 9, Paper 2.3
Civil-Comp Press, Edinburgh, United Kingdom, 2024
ISSN: 2753-3239, doi: 10.4203/ccc.9.2.3

The Influence of Unit Cell Design on the Mechanical Properties of Ti6Al4V Lattice Structures Fabricated via Laser Powder Bed Fusion

M. Casata[1], D. Patil[1,2] and D. Barba[1]

[1] E.T.S. de Ingeniería Aeronáutica y del Espacio, Universidad Politécnica de Madrid, Madrid, Spain
[2] Alloyed Ltd, Alloyed Ltd, Yarnton, United Kingdom

Abstract

The laser powder bed fusion process enables the manufacturing of intricate shapes, including lattice structure metamaterials. These lattice structures consist of repeating unit cells, formed by nodes connected by struts within space. In this study, various unit cell designs were fabricated in Ti6Al4V, maintaining consistent relative density, and subsequently were tested under uniaxial compression loading. The results highlight differences in mechanical responses and failure mechanisms between the lattice designs. The findings reveal that face-centered cubic exhibits better mechanical properties, including yield stress, elastic modulus, peak stress, and absorbed energy, in comparison to body-centered cubic structures. This study provides valuable insights into optimizing lattice structure design for enhanced mechanical performance in LPBF-fabricated Ti6Al4V components.

Keywords: LPBF, metamaterials, lattice structures, mechanical properties, failure mechanism, CAD deviation

1 Introduction

Laser powder bed fusion (LPBF) process represents a revolutionary paradigm in additive manufacturing, distinguished by its ability to produce intricate geometries with unparalleled precision [1]. This method requires the selective fusion of powdered materials, utilizing a high-energy laser beam layer-by-layer. LPBF process facilitates the fabrication of intricate structures boasting extraordinary detail and accuracy by controlling the laser's trajectory and intensity. Initially conceived for rapid prototyping and limited-scale production, LPBF process has undergone a transformative evolution, emerging as a versatile manufacturing technique with widespread applications across diverse industries, including aerospace, automotive, healthcare, and electronics [2]. Given its ability to produce complex-shaped parts, LPBF process offers many advantages when producing complex-shaped metamaterials. Metamaterials are engineered materials offering substantial mechanical properties and advantages, potentially transforming engineering applications. They can be engineered with customized elasticity, unique auxetic behavior, gradient mechanical properties, and adaptable responses to external stimuli [3]. Metamaterials achieve exceptional strength-to-weight ratios by optimizing microstructure and composition, rendering them suitable for lightweight yet durable structures. In metamaterials, a lattice structure refers to a repeating geometric pattern formed by interconnected structural elements in the 3D space. [4] The lattice structure in metamaterials is often characterized by its periodicity, symmetry, and unit cell geometry. Different types of lattice structures, such as cubic, hexagonal, or diamond, can be employed depending on the desired mechanical properties of the metamaterial. Metamaterials can be broadly distinguished topologically based on whether they undergo stretching or bending under the influence of external force [5]. Bending-dominated and stretching-dominated deformation mechanisms represent distinct modes of deformation exhibited by 3D-printed metal lattice structures when subjected to external loads. Bending-dominated lattice structures exhibit inferior mechanical strength yet demonstrate superior energy absorption properties [6]. The elastic strain energy stored within these bending struts is comparatively minimal upon the initiation of plasticity or failure [6]. With an increase in the relative density of bending-dominated lattices, deformation transitions from pure bending to a combination of bending, stretching, and shear [6]. This transition towards increased stretching and shear deformation may induce post-yield softening (PYS) behavior. Conversely, stretching-dominated lattice configurations manifest higher modulus and yield strength than their bending-dominated counterparts [7]. Within stretching-dominated lattices, deformation occurs primarily through axial stretching or compression of lattice struts. The elastic strain energy stored within these stretching struts is significantly more pronounced upon the onset of plasticity or failure [7]. The abrupt release of this stored elastic strain energy during plastic deformation can engender post-yield softening (PYS) behavior within stretching-dominated lattices [8].

The research proposed in this study aims to study the mechanical response of different lattice structures presenting stretching-dominated and bending-dominated behaviors, printed in Ti6Al4V by LPBF under quasi-static compression loading. The

lattices' yield stress, elastic modulus, energy absorption, and the study of their failure mode were studied and compared.

2 Methods

This section briefly discusses the materials, the lattice structure design, manufacturing, and the testing carried out in this study.

2.1 Materials and Manufacturing Process

The material chosen for this study was Ti6Al4V ELI provided by Carpenter Additive® with a powder size distribution ranging from 14.9 μm (D10) to 53.6 μm (D90). The lattice structures were produced via LPBF process using an Aconity Mini® equipped with a 400 W laser. A laser power of 129 W, scan speed of 1001 mm/s, hatch spacing of 74 μm and a spot size of 80 μm were chosen to manufacture the lattices. A contour-hatch scan strategy applying a rotation of 67°each layer was used. These processing parameters ensure that fully dense ($< 99.5\%$) struts are produced based on previous studies.

2.2 Lattice Structure Design

As part of this study, six different types of strut-based lattice structures (3x3x4 unit cells) were selected for testing. These include Cubic (cubic), Face-centered cubic (FCC), Diamond (diam), Body-centered cubic (BCC), Graded BCC 1 (Gr1), and Graded BCC 2 (Gr2) lattice structures, illustrated in Figure 1.

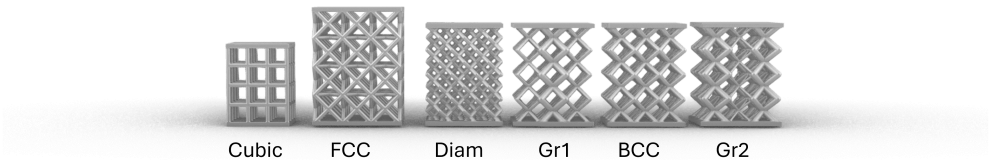

Figure 1: Schematic representation of the lattice structures considered for this analysis. Six different unit cells were considered: Diam, Gr1, Gr2, BCC, cubic, FCC.

To achieve a target relative density of 20%, a fixed diameter of 1 mm was maintained for Cubic, FCC, Diam, and BCC lattice structures, while the unit cell size was varied. Conversely, for Gr1 and Gr2 structures, the same unit cell size as BCC was retained, and the strut diameter was adjusted. Two distinct patterns were employed to

modify the diameter, as illustrated in Figure 2. Gr1 and Gr2 alternative lattice designs were implemented to assess the influence of different strut diameter configurations on the mechanical response and failure mode compared to conventional BCC designs.

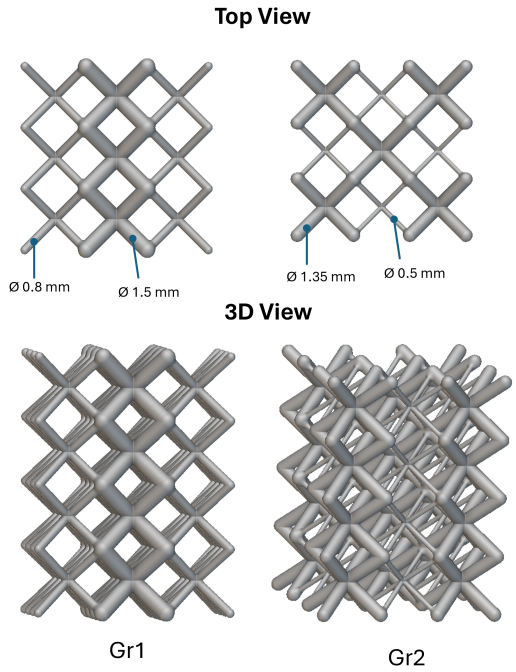

Figure 2: Schematic representation of the Gr1 and Gr2 designs considered for this analysis. Different thickening patterns of strut diameters were implemented.

2.3 Mechanical Testing and Characterization

Uniaxial compression tests were performed on a universal servo-hydraulic test machine equipped with a 100 kN load cell. The compression test was conducted at a constant strain rate of $10^{-2}1/s$. The strain was measured by DIC software (Digital Imaging Correlation). For each test, the yield stress (YS), peak strength (PS) calculated as the first peak after the elastic phase, elastic modulus (E), and the absorbed energy (AE) per unit volume were calculated.

3 Results

This section highlights the mechanical properties of the lattices obtained after uniaxial compression testing and assesses their failure modes. It aims to compare and rationalize their different responses.

According to Maxwell's stability criterion, all the lattices investigated in this study pertain to the bending-dominated topology category [9], however, previous studies have shown that cubic and FCC lattices may behave as stretching-dominated structures under uniaxial compression load [10, 11]. To facilitate a comprehensive analysis, lattices exhibiting bending-dominated behavior were studied separately from those demonstrating stretching-dominated behavior. At the end of this section, a comparison of the responses of all the lattices was presented.

The stress-strain curves of lattice structures subjected to quasi-static compression tests can be divided into three main regions: i) a linear elastic regime, ii) an inelastic regime, and iii) a densification phase [12, 13]. As part of this study, only the stress-strain curves up to the first stress drop were analyzed. This decision was made because the densification phase lies beyond the scope of this study. Furthermore, the intended applications for these lattices primarily involve operations within the elastic region. The nominal stress-strain curves of the lattice structures presenting a bending-dominated behavior are reported in Figures 3. All the curves shown in Figure 3 exhibit similar elastic behavior, with minor discrepancies appearing in the inelastic region after reaching the yield stress. Specifically, BCC, Gr1, and Gr2 lattices display a longer stress plateau, whereas the diamond unit cell lattice shows a consistent stress decrease. These stress plateaus are characteristic of bending-dominated structures, a well-documented phenomenon documented in literature [10, 12, 13].

The failure mode of the bending-dominated lattices is illustrated in Figure 4, depicting a comparison of each lattice before deformation and after the stress drop. Despite the different arrangements of the connection in the diamond lattice structure compared to the BCC one, and the different strut aspect ratio used in Gr1 and Gr2, the same failure mechanism was observed across the lattices: after an initial homogeneous deformation during the elastic region, strain localization occurs following the yield stress, leading to failure by forming 45°shear bands. Zhong et al. [6] have observed that this phenomenon is prevalent in bending-dominated lattices when printed at high relative densities. At such densities, the stretching and the shear contributions to deformation increase, resulting in oriented crushing at approximately 45°angles [6]. This finding, combined with the results obtained by testing different unit cells with the same relative densities, suggests that the relative density is the driving factor of such a failure mechanism independently of the unit cell design.

The nominal stress-strain curves of cubic and FCC lattices are depicted in Figure 5. These structures exhibit higher stiffness and yield stress compared to their bending-dominated counterparts. In the case of cubic lattices, the elastic region is followed by a sharp post-yield softening, resulting in a rapid decrease in mechanical properties. Conversely, FCC lattices display a smoother post-yield softening compared to cubic ones, albeit still sharper than observed in bending-dominated lattices.

The different behavior between the two unit cells is observed in the deformed frames of the lattices represented in Figure 6. Within the inelastic region of Cubic cell lattices, the deformation occurs layer-by-layer due to the buckling of the vertical struts. This layer crush results in a sudden release of elastic strain, translating into a

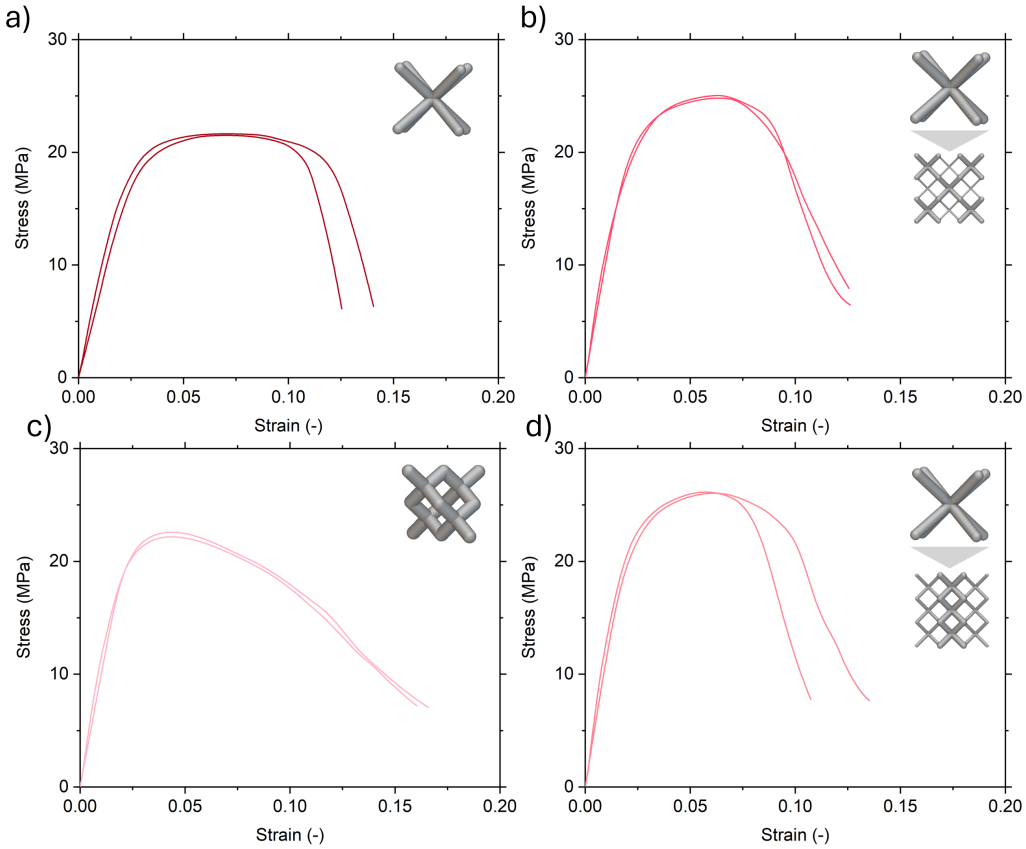

Figure 3: Stress-strain curves of the bending-dominated lattice structures a) BCC, b) Gr1, c) Diam, d) Gr2 tested under compression.

steep post-yield softening [6, 12]. On the other hand, FCC structures present a mixed post-yielding behavior that can be observed in Figure 6 b. Both layer-by-layer crushing and shear band formation at 45°are observed during deformation. Similar behavior was observed by Banait et al. [11] when testing a FCC structure in Inconel718, resulting in a stress peak phenomenon after yielding followed by a stress plateau characteristic of the bending-dominated behavior lattices. This phenomenon may be attributed to the coupling of different deformation mechanisms such as plastic hinging at the nodes and buckling of the struts simultaneously [11].

The main mechanical properties extracted from the compression tests, namely yield stress, PS, Elastic Modulus, and absorbed energy are reported in Figure 7. As expected and previously reported [12, 13], the structures with a stretching-dominated behavior, namely Cubic and FCC, have overall higher yield stress, stiffness, and PS than their bending-dominated counterparts. In particular, Cubic structures present an increase of 282%, 672%, and 180% in yield stress, Elastic Modulus, and Peak stress, respec-

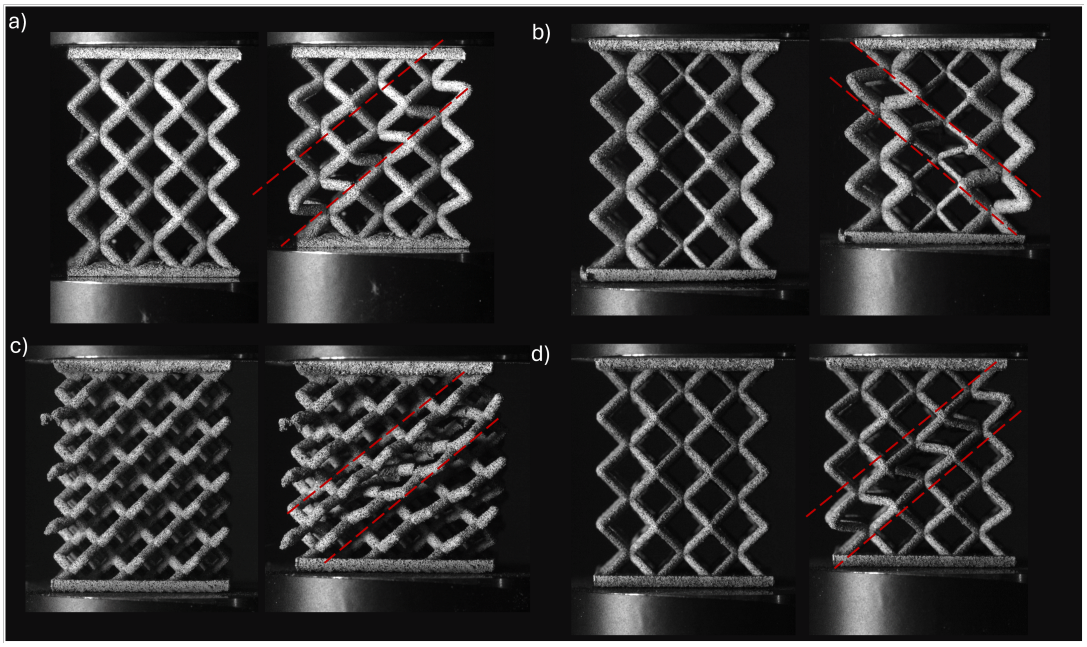

Figure 4: The undeformed and deformed configuration of the lattices including a) BCC, b) Gr1, c) diam, d) Gr2 ere examined during quasi-static compression testing. 45°shear bands (in red) is the main failure mechanism for all the tested lattices.

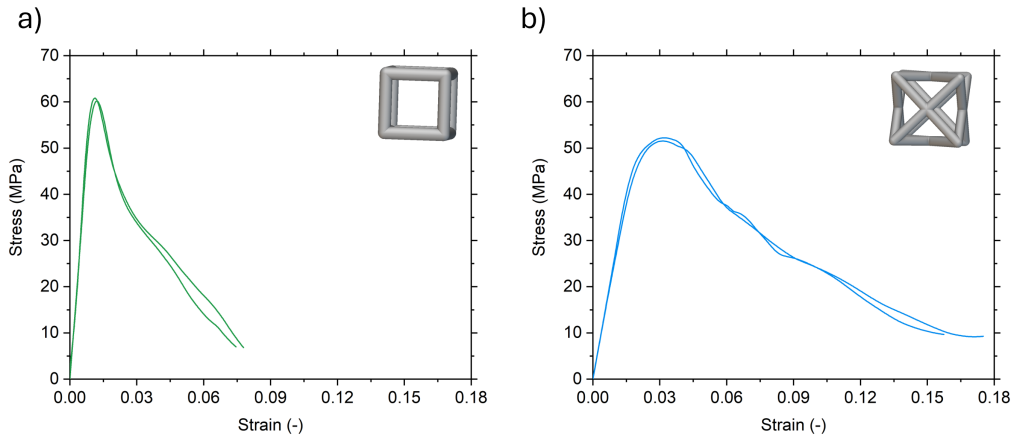

Figure 5: Stress-strain curves of the lattice structures a) Cubic, b) FCC tested under compression. Both lattices present a stretching-dominated behavior despite being classified as bending-dominated according to Maxwell stability criterion.

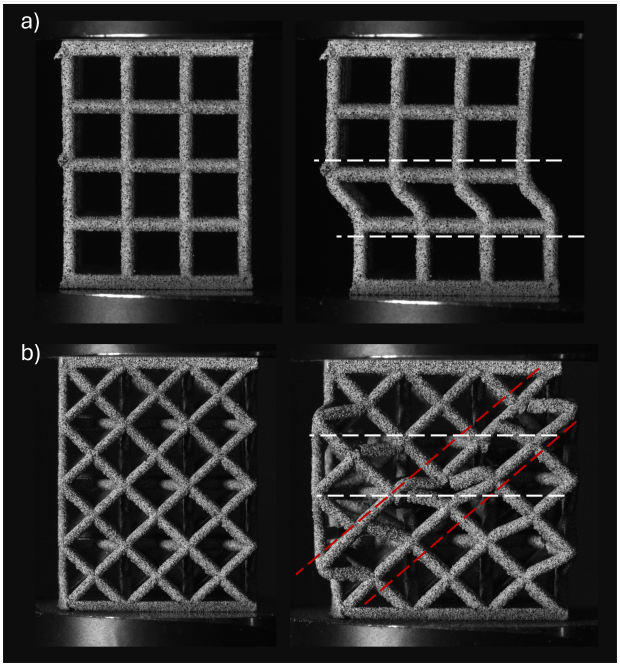

Figure 6: The undeformed and deformed configurations of the lattice structures, including (a) FCC and (b) Cubic, were examined during quasi-static compression testing. Notably, 45°shear bands, depicted in red, emerged in the deformed structures, indicating localized strain. The layer-by-layer deformation caused by buckling is highlighted in white, emphasizing the structural response to compression forces.

tively, compared to BCC structures, while only a 6% decrease in Absorbed energy was registered. The elevated mechanical properties of the Cubic cell are attributed to the ability of the vertical strut to withstand the axial load during compression, which is different from the bending load experienced by the diagonal struts in BCC. Only a marginal increase in the mechanical properties was observed for Gr1 and Gr2 compared to BCC, with the former outperforming Gr2. This change may be attributed to the different mechanical properties of the strut at different dimensions [14, 15]. This difference in the mechanical properties may lead to a different macro-response in the lattice. Finally, FCC structures exhibit higher yield stress, plastic strain, and elastic modulus, compared to BCC ones. Additionally, they demonstrate a two-fold increase in absorbed energy. This finding suggests that the FCC unit cell design is well-suited for energy absorption applications, despite its partially stretching-dominated behavior. This is particularly significant as the low yield stress of bending-dominated lattice structures may limit their ability to absorb energy effectively.

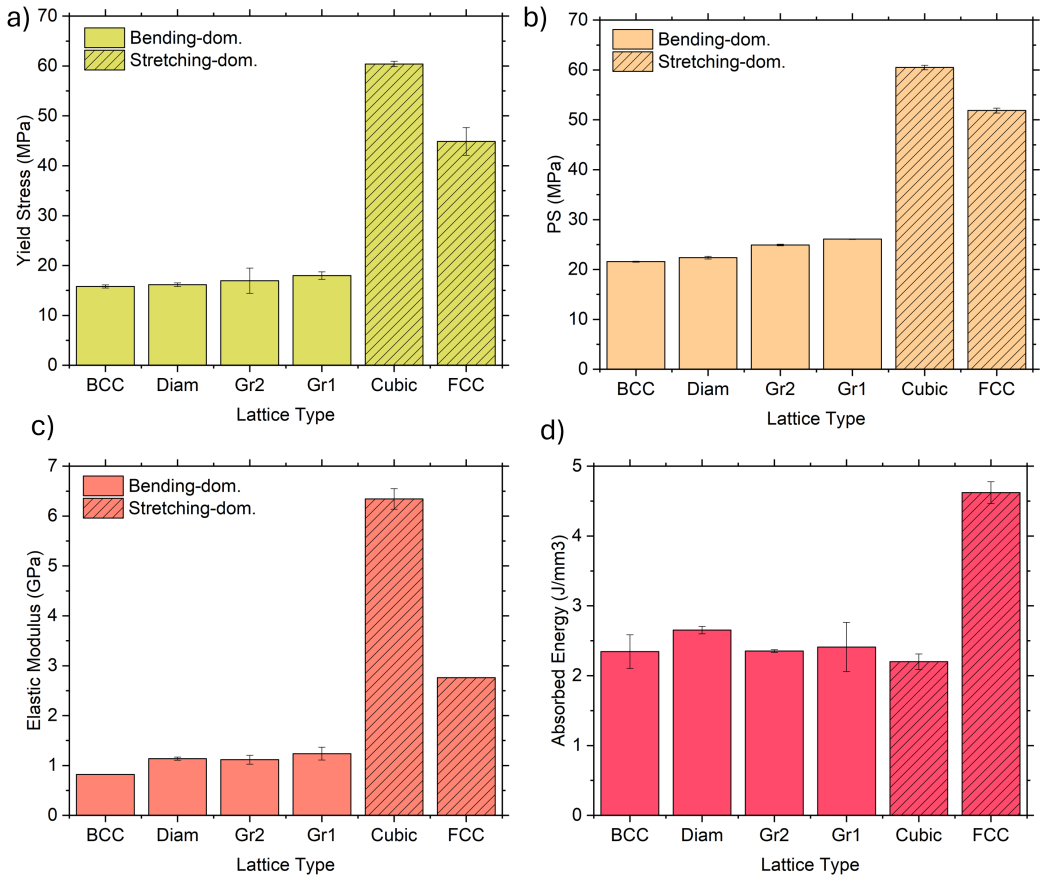

Figure 7: Comparison of the uniaxial compression mechanical properties of the different lattice structures tested. a) yield stress, b) peak stress, c) elastic modulus, and absorbed energy .

4 Concluding remarks

This study investigated the mechanical properties under uniaxial compression loading of different Ti6Al4V lattice structures printed using various unit cell designs and strut diameters while maintaining the same relative density. All the lattices were printed without any visible defects. From the mechanical properties and the failure mode analysis the following conclusions can be drawn:

- BCC, diamond, Gr1, and Gr2 lattice structures exhibited bending-dominated behavior, with similar values of yield stress, peak stress, elastic modulus, and absorbed energy.
- Despite being classified as bending-dominated by Maxwell's criterion, Cubic lattices behaved as stretching-dominated structures, showing elevated stiffness and yield stress but experiencing a sharp drop in mechanical properties after yielding.
- FCC lattices displayed mixed properties from both stretching and bending-dominated

lattices, with a mixed failure mechanism observed, allowing them to maintain elevated stiffness and yield stress while improving energy absorption compared to other bending-dominated lattices.

Overall, FCC lattices were identified as the most suitable unit cell design among those studied due to their mixed properties and improved energy absorption capabilities.

Acknowledgements

This project has received funding from the European Union's Horizon 2020 research and innovation programme under the Marie Skłodowska-Curie grant agreement No 956401.

Grant EQC2019-006491-P funded by MICIU/AEI/10.13039/501100011033 and by ERDF A way of making Europe.

References

[1] R. Singh, A. Gupta, O. Tripathi, S. Srivastava, B. Singh, A. Awasthi, S. K. Rajput, P. Sonia, P. Singhal, K. K. Saxena, Powder bed fusion process in additive manufacturing: An overview, Vol. 26, Elsevier Ltd, 2019, pp. 3058–3070. doi:10.1016/j.matpr.2020.02.635.

[2] T. DebRoy, H. L. Wei, J. S. Zuback, T. Mukherjee, J. W. Elmer, J. O. Milewski, A. M. Beese, A. Wilson-Heid, A. De, W. Zhang, Additive manufacturing of metallic components – process, structure and properties (3 2018). doi:10.1016/j.pmatsci.2017.10.001.

[3] X. Zhou, L. Ren, Z. Song, G. Li, J. Zhang, B. Li, Q. Wu, W. Li, L. Ren, Q. Liu, Advances in 3d/4d printing of mechanical metamaterials: From manufacturing to applications (4 2023). doi:10.1016/j.compositesb.2023.110585.

[4] Z. Jia, F. Liu, X. Jiang, L. Wang, Engineering lattice metamaterials for extreme property, programmability, and multifunctionality (4 2020). doi:10.1063/5.0004724.

[5] Y. Zhang, Y. Pan, D. Han, W. Z. Jiang, W. Jiang, X. G. Zhang, X. C. Teng, X. H. Ni, X. Ren, A hybrid design for bending and stretching dominated metamaterial with tailorable thermal expansion, Composite Structures 323 (11 2023). doi:10.1016/j.compstruct.2023.117474.

[6] H. Z. Zhong, C. W. Li, R. Das, J. F. Gu, M. Qian, Post-yield softening of bending-dominated metal metamaterials, PNAS Nexus 2 (3 2023). doi:10.1093/pnasnexus/pgad075.

[7] L. Riva, P. S. Ginestra, E. Ceretti, Mechanical characterization and properties of laser-based powder bed-fused lattice structures: a reviewdoi:10.1007/s00170-021-06631-4/Published.
URL https://doi.org/10.1007/s00170-021-06631-4

[8] B. Khoda, A. M. Ahsan, A. N. Shovon, A. I. Alam, 3d metal lattice structure manufacturing with continuous rods, Scientific Reports 11 (12 2021). doi:10.1038/s41598-020-79826-6.

[9] V. S. Deshpande, M. F. Ashby, N. A. Fleck, Foam topology bending versus stretching dominated architectures (2001).
URL www.elsevier.com/locate/actamat

[10] J. Kadkhodapour, H. Montazerian, A. C. Darabi, A. P. Anaraki, S. M. Ahmadi, A. A. Zadpoor, S. Schmauder, Failure mechanisms of additively manufactured porous biomaterials: Effects of porosity and type of unit cell, Journal of the Mechanical Behavior of Biomedical Materials 50 (2015) 180–191. doi:10.1016/j.jmbbm.2015.06.012.

[11] S. Banait, C. Liu, M. Campos, M. S. Pham, M. T. Pérez-Prado, Coupled effect of microstructure and topology on the mechanical behavior of inconel718 additively manufactured lattices, Materials and Design 224 (12 2022). doi:10.1016/j.matdes.2022.111294.

[12] M. Benedetti, A. du Plessis, R. O. Ritchie, M. Dallago, N. Razavi, F. Berto, Architected cellular materials: A review on their mechanical properties towards fatigue-tolerant design and fabrication (4 2021). doi:10.1016/j.mser.2021.100606.

[13] C. Intrigila, N. A. Nodargi, P. Bisegna, The compressive response of additively-manufactured hollow truss lattices: an experimental investigation, International Journal of Advanced Manufacturing Technology 120 (2022) 3529–3541. doi:10.1007/s00170-022-08716-0.

[14] D. Barba, C. Alabort, Y. T. Tang, M. J. Viscasillas, R. C. Reed, E. Alabort, On the size and orientation effect in additive manufactured ti-6al-4v, Materials and Design 186 (1 2020). doi:10.1016/j.matdes.2019.108235.

[15] U. Hossain, S. Ghouse, K. Nai, J. R. Jeffers, Mechanical and morphological properties of additively manufactured ss316l and ti6al4v micro-struts as a function of build angle, Additive Manufacturing 46 (2021) 102050. doi:10.1016/j.addma.2021.102050.